Supporting information for "*PlanetProfile:* Self-consistent interior structure modeling for terrestrial bodies in Python"

M. J. Styczinski[1,2], S. D. Vance[2], and M. Melwani Daswani[2]

[1]NASA Postdoctoral Program Fellow, Jet Propulsion Laboratory, California Institute of Technology, Pasadena, California, USA

[2]Jet Propulsion Laboratory, California Institute of Technology, Pasadena, California, USA

Contents of this file

Introduction

This supplement contains comparisons between models of major moons generated with the latest version of *PlanetProfile* (v2.3.3, Styczinski et al., 2022) and analogous models from Vance et al. (2018), generated with the initial Matlab release of *PlanetProfile* (v1.0.0, Vance, 2017). The models we include here incorporate new features for improved self-consistency as described in the main text. An $H_2O–NH_3$ EOS has not yet been implemented in the Python version of *PlanetProfile*, so those models are omitted from the comparison.

Text S1.

Figures S1 – S5 compare several models of the moons Europa, Ganymede, Callisto, Enceladus, and Titan, as studied in Vance et al. (2018). Tables S1 – S5 summarize the same models as those presented in the corresponding figures. Input Python files used to generate these figures and tables, output text files describing layer properties and model summaries, and comparison figure files are available as a Zenodo share at `https://doi.org/10.5281/zenodo.7318029`.

The models in this supplement have been adjusted from the default models described in the main text, with adjustments to the ocean melting temperature T_b such that the ice shell thickness z_b matches the models from Vance et al. (2018) as closely as possible. For some porous models, further adjustments were sometimes required in order to construct a valid model. In order to match the MoI for Titan and Callisto, we had to use extremely high rock porosities ϕ_{rock} and pore closure pressures $P_{c,\mathrm{rock}}$. This implies that the published MoI values for these bodies may be too high (due to a non-hydrostatic configuration) and a more realistic model for the required very-low-density rocky mantle will be important in future study. The configurations required to find MoI that lie within the uncertainty bounds as described in Section 1.1 imply that Titan and Callisto are not fully differentiated. A wider parameter space of models fits with the MoI for thinner ice shells, because the ocean density varies with the dissolved salt content, but the ice shell density does not. The low density of the ice shell drives down the MoI, adding tighter constraints on other parameters to match the high MoI for these bodies.

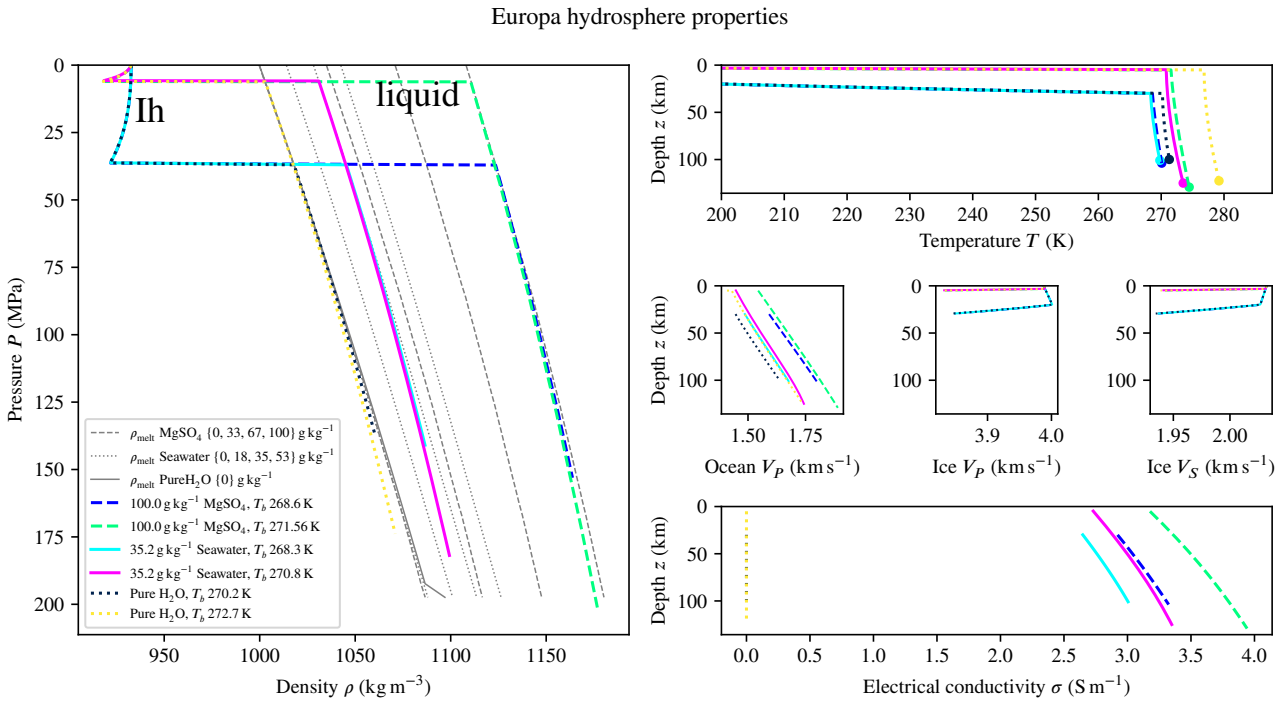

Figure S1. Updated *PlanetProfile* outputs for Europa, modeled after the conditions studied by Vance et al. (2018). Compare to Figure 7 from Vance et al. Refer to Table 5 (main text) for variable definitions.

	Europa	**Europa**	**Europa**	**Europa**	**Europa**	**Europa**
Ocean comp.	100.0 g kg^{-1} $MgSO_4$	100.0 g kg^{-1} $MgSO_4$	35.2 g kg^{-1} Seawater	35.2 g kg^{-1} Seawater	Pure H_2O	Pure H_2O
M(kg)	4.8000×10^{22}	4.8000×10^{22}	4.8000×10^{22}	4.8000×10^{22}	4.8000×10^{22}	4.8000×10^{22}
M_{model}(kg)	4.7926×10^{22}	4.7976×10^{22}	4.7955×10^{22}	4.7941×10^{22}	4.7965×10^{22}	4.7939×10^{22}
C/MR^2	0.346 ± 0.005	0.346 ± 0.005	0.346 ± 0.005	0.346 ± 0.005	0.346 ± 0.005	0.346 ± 0.005
C_{model}/MR^2	$0.34600^{+0.00042}_{-0.00042}$	$0.34606^{+0.00022}_{-0.00040}$	$0.34605^{+0.00047}_{-0.00047}$	$0.34618^{+0.00043}_{-0.00043}$	$0.34605^{+0.00026}_{-0.00048}$	$0.34601^{+0.00046}_{-0.00028}$
$\rho_{\text{rock,mean}}$(kg m^{-3})	3294	3436	3295	3443	3295	3438
T_b(K)	268.6	271.56	268.3	270.8	270.2	272.7
q_{surf}(mW m^{-2})	16.1	98.2	16.1	103.2	16.2	99.5
q_{con}(mW m^{-2})	16.7	98.8	16.8	103.9	16.9	100.1
η_{con}(Pa s)	3.38×10^{14}	2.82×10^{14}	3.49×10^{14}	3.05×10^{14}	2.87×10^{14}	2.51×10^{14}
D_{lh}(km)	30.0	5.1	29.9	4.8	30.0	5.0
D_{ocean}(km)	74.4	124.8	71.6	120.8	70.6	118.2
$\overline{\sigma}_{\text{ocean}}$(S m^{-1})	3.1	3.6	2.8	3.1	0.0	0.0
R_{surf}(km)	1560.8	1560.8	1560.8	1560.8	1560.8	1560.8
R_{rock}(km)	1456.4	1431.0	1459.3	1435.2	1460.2	1437.6
R_{core}(km)	594.7	572.4	595.9	562.1	596.3	563.0

Table S1. Updated *PlanetProfile* outputs for Europa, modeled after the conditions studied by Vance et al. (2018). Compare to Table 6 from Vance et al. Refer to Table 5 (main text) for variable definitions.

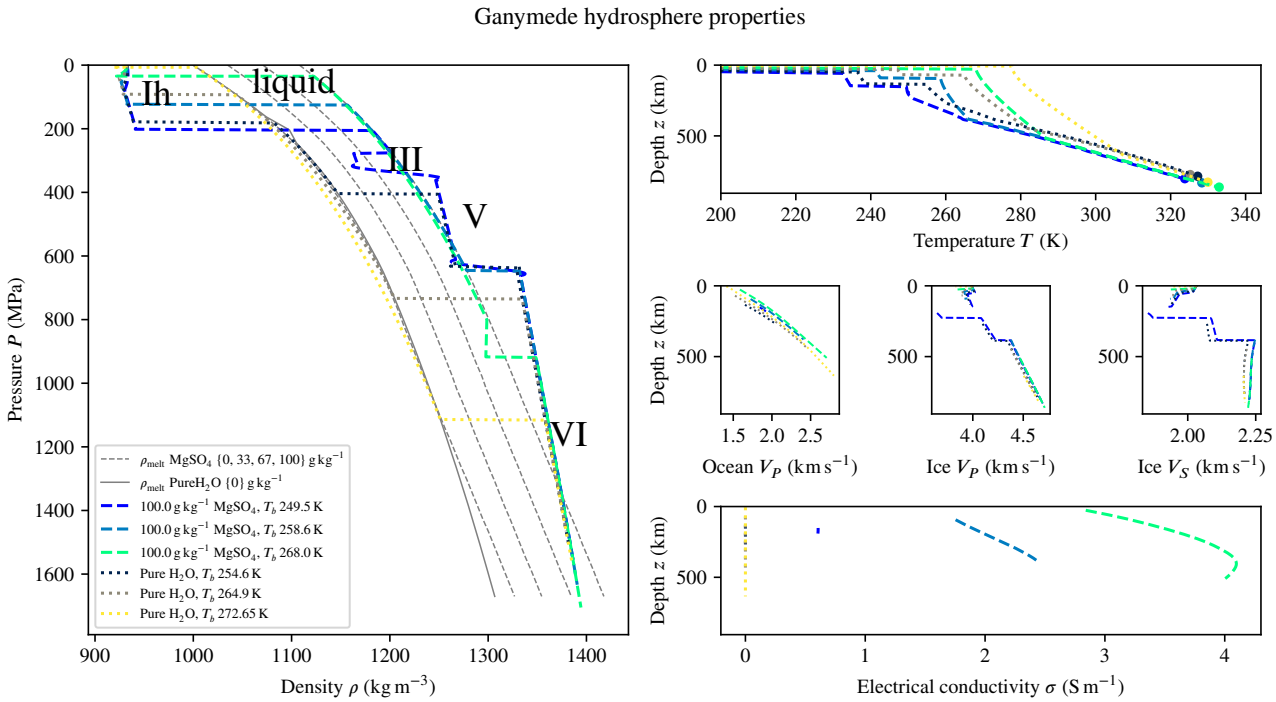

Figure S2. Updated *PlanetProfile* outputs for Ganymede, modeled after the conditions studied by Vance et al. (2018). Compare to Figure 5 from Vance et al. Refer to Table 5 (main text) for variable definitions.

	Ganymede	**Ganymede**	**Ganymede**	**Ganymede**	**Ganymede**	**Ganymede**
Ocean comp.	100.0 g kg^{-1} $MgSO_4$	100.0 g kg^{-1} $MgSO_4$	100.0 g kg^{-1} $MgSO_4$	Pure H_2O	Pure H_2O	Pure H_2O
M(kg)	1.4819×10^{23}	1.4819×10^{23}	1.4819×10^{23}	1.4819×10^{23}	1.4819×10^{23}	1.4819×10^{23}
M_{model}(kg)	1.4798×10^{23}	1.4805×10^{23}	1.4794×10^{23}	1.4804×10^{23}	1.4812×10^{23}	1.4818×10^{23}
C/MR^2	0.3115 ± 0.0028	0.3115 ± 0.0028	0.3115 ± 0.0028	0.3115 ± 0.0028	0.3115 ± 0.0028	0.3115 ± 0.0028
C_{model}/MR^2	$0.31148^{+0.00014}_{-0.00006}$	$0.31155^{+0.00013}_{-0.00013}$	$0.31151^{+0.00012}_{-0.00009}$	$0.31156^{+0.00014}_{-0.00014}$	$0.31146^{+0.00014}_{-0.00014}$	$0.31152^{+0.00014}_{-0.00015}$
$\rho_{\text{rock,mean}}$(kg m^{-3})	3234	3220	3215	3226	3205	3551
T_b(K)	249.5	258.6	268.0	254.6	264.9	272.65
q_{surf}(mW m^{-2})	10.4	16.5	18.4	13.2	22.4	97.7
q_{con}(mW m^{-2})	11.7	17.7	18.8	14.7	23.7	98.1
η_{con}(Pa s)	1.34×10^{15}	6.82×10^{14}	3.63×10^{14}	8.10×10^{14}	3.92×10^{14}	2.52×10^{14}
D_{Ih}(km)	151.4	93.4	26.4	134.3	69.8	5.1
D_{ocean}(km)	40.7	287.0	483.6	134.4	375.7	630.9
D_{III}(km)	34.4	-	-	-	-	-
D_{V}(km)	157.6	-	-	119.7	-	-
D_{VI}(km)	419.2	452.2	352.9	397.7	328.7	192.0
$\overline{\sigma}_{\text{ocean}}$(S m^{-1})	0.6	2.1	3.8	0.0	0.0	0.0
R_{surf}(km)	2631.2	2631.2	2631.2	2631.2	2631.2	2631.2
R_{rock}(km)	1828.0	1798.7	1768.3	1845.1	1857.0	1803.1
R_{core}(km)	655.0	734.5	795.7	630.4	650.0	285.5

Table S2. Updated *PlanetProfile* outputs for Ganymede, modeled after the conditions studied by Vance et al. (2018). Compare to Table 5 from Vance et al. Refer to Table 5 (main text) for variable definitions.

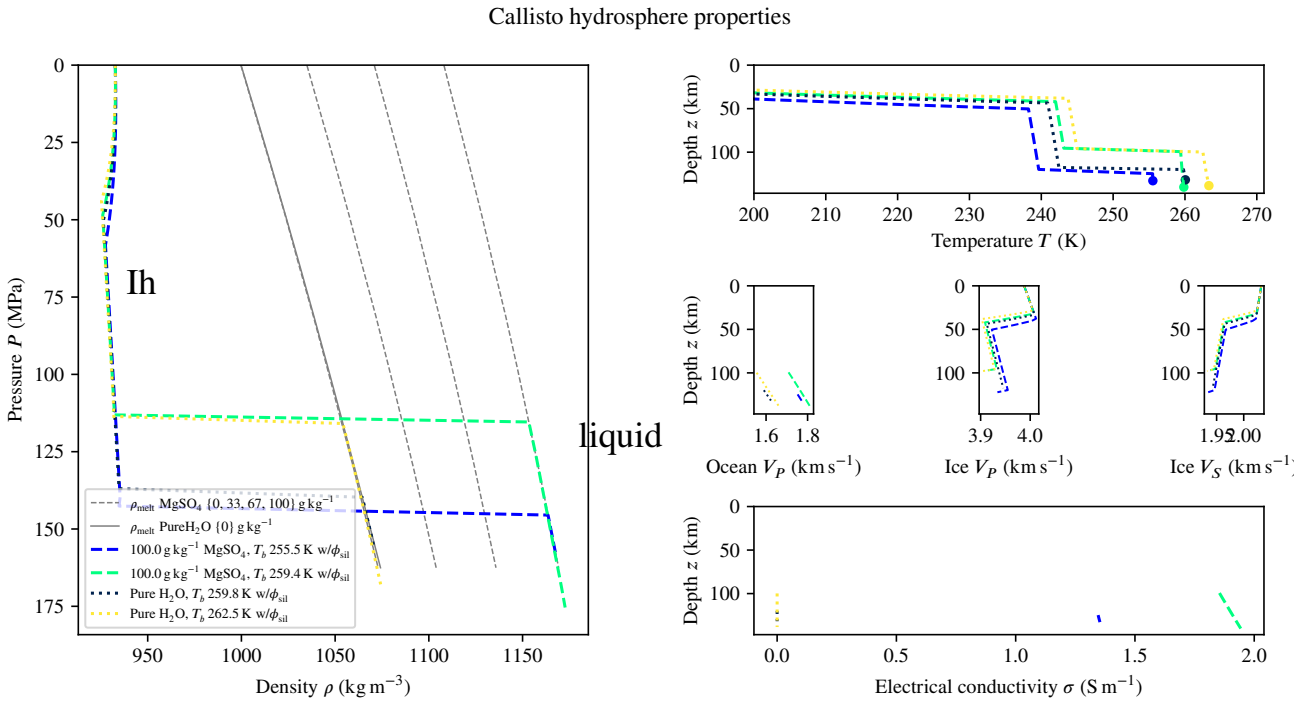

Figure S3. Updated *PlanetProfile* outputs for Callisto, modeled after the conditions studied by Vance et al. (2018). Compare to Figure 14 from Vance et al. Refer to Table 5 (main text) for variable definitions.

	Callisto	**Callisto**	**Callisto**	**Callisto**
Ocean comp.	$100.0\,\mathrm{g\,kg^{-1}}$ $MgSO_4$	$100.0\,\mathrm{g\,kg^{-1}}$ $MgSO_4$	Pure H_2O	Pure H_2O
M(kg)	1.0759×10^{23}	1.0759×10^{23}	1.0759×10^{23}	1.0759×10^{23}
M_{model}(kg)	1.0756×10^{23}	1.0759×10^{23}	1.0757×10^{23}	1.0756×10^{23}
C/MR^2	$0.3549^{+0.0042}_{-0.0148}$	$0.3549^{+0.0042}_{-0.0148}$	$0.3549^{+0.0060}_{-0.0166}$	$0.3549^{+0.0060}_{-0.0166}$
C_{model}/MR^2	$0.34147^{+0.00000}_{-0.00000}$	$0.34216^{+0.00000}_{-0.00202}$	$0.33842^{+0.00000}_{-0.00000}$	$0.33852^{+0.00000}_{-0.00000}$
$\rho_{\mathrm{rock,mean}}(\mathrm{kg\,m^{-3}})$	2000	2001	2000	2004
T_b(K)	255.5	259.4	259.8	262.5
$q_{\mathrm{surf}}(\mathrm{mW\,m^{-2}})$	12.9	15.8	15.6	18.0
$q_{\mathrm{con}}(\mathrm{mW\,m^{-2}})$	14.3	17.2	17.3	19.6
$\eta_{\mathrm{con}}(\mathrm{Pa\,s})$	8.90×10^{14}	6.53×10^{14}	5.50×10^{14}	4.58×10^{14}
D_{lh}(km)	124.7	99.4	119.9	99.8
D_{ocean}(km)	9.5	42.1	13.3	40.1
$\overline{\sigma}_{\mathrm{ocean}}(\mathrm{S\,m^{-1}})$	1.3	1.9	0.0	0.0
R_{surf}(km)	2410.3	2410.3	2410.3	2410.3
R_{rock}(km)	2276.1	2268.8	2277.1	2270.4
ϕ_{rock}	0.99	0.99	0.99	0.99

Table S3. Updated *PlanetProfile* outputs for Callisto, modeled after the conditions studied by Vance et al. (2018). Compare to Table 10 from Vance et al. Refer to Table 5 (main text) for variable definitions.

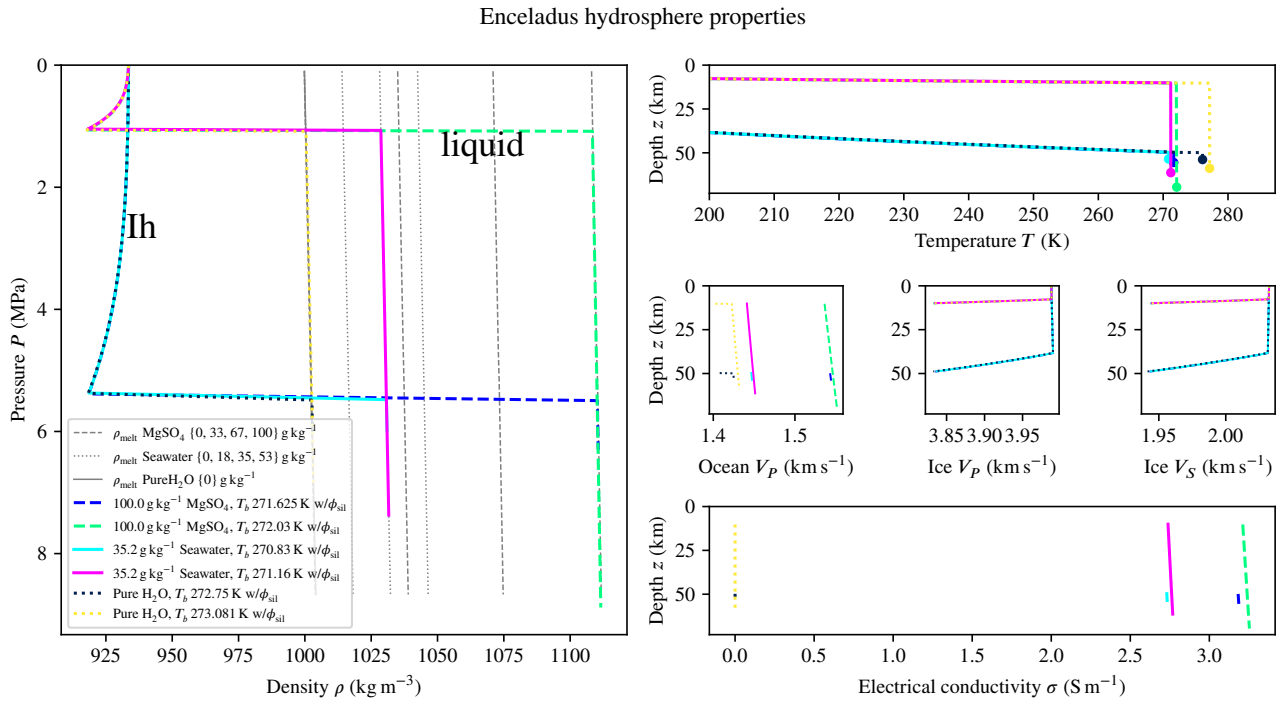

Figure S4. Updated *PlanetProfile* outputs for Enceladus, modeled after the conditions studied by Vance et al. (2018). Compare to Figure 10 from Vance et al. Refer to Table 5 (main text) for variable definitions.

	Enceladus	**Enceladus**	**Enceladus**	**Enceladus**	**Enceladus**	**Enceladus**
Ocean comp.	100.0 g kg^{-1} $MgSO_4$	100.0 g kg^{-1} $MgSO_4$	35.2 g kg^{-1} Seawater	35.2 g kg^{-1} Seawater	Pure H_2O	Pure H_2O
M(kg)	1.0802×10^{20}	1.0802×10^{20}	1.0802×10^{20}	1.0802×10^{20}	1.0802×10^{20}	1.0802×10^{20}
$M_{\rm model}$(kg)	1.0801×10^{20}	1.0769×10^{20}	1.0800×10^{20}	1.0769×10^{20}	1.0766×10^{20}	1.0755×10^{20}
C/MR^2	0.335 ± 0.001	0.335 ± 0.001	0.335 ± 0.001	0.335 ± 0.001	0.335 ± 0.001	0.335 ± 0.001
$C_{\rm model}/MR^2$	$0.33434^{+0.00136}_{-0.00006}$	$0.33459^{+0.00000}_{-0.00000}$	$0.33565^{+0.00000}_{-0.00154}$	$0.33445^{+0.00000}_{-0.00000}$	$0.33444^{+0.00000}_{-0.00007}$	$0.33409^{+0.00000}_{-0.00000}$
$\rho_{\rm rock,mean}$(kg m^{-3})	2360	2485	2329	2399	2327	2371
T_b(K)	271.625	272.03	270.83	271.16	272.75	273.081
$q_{\rm surf}$(mW m^{-2})	9.3	47.4	9.3	47.9	9.4	47.4
$q_{\rm con}$(mW m^{-2})	14.5	51.5	14.5	52.0	14.5	51.5
$\eta_{\rm con}$(Pa s)	2.54×10^{14}	2.48×10^{14}	2.75×10^{14}	2.71×10^{14}	2.27×10^{14}	2.24×10^{14}
$D_{\rm lh}$(km)	49.9	10.2	49.7	10.1	49.8	10.2
$D_{\rm ocean}$(km)	6.4	60.1	4.6	52.0	4.9	49.4
$\overline{\sigma}_{\rm ocean}$(S m^{-1})	3.2	3.2	2.7	2.8	0.0	0.0
$R_{\rm surf}$(km)	252.1	252.1	252.1	252.1	252.1	252.1
$R_{\rm rock}$(km)	195.9	181.8	197.8	190.0	197.5	192.5
$\phi_{\rm rock}$	0.27	0.27	0.27	0.32	0.32	0.32

Table S4. Updated *PlanetProfile* outputs for Enceladus, modeled after the conditions studied by Vance et al. (2018). Compare to Table 7 from Vance et al. Refer to Table 5 (main text) for variable definitions.

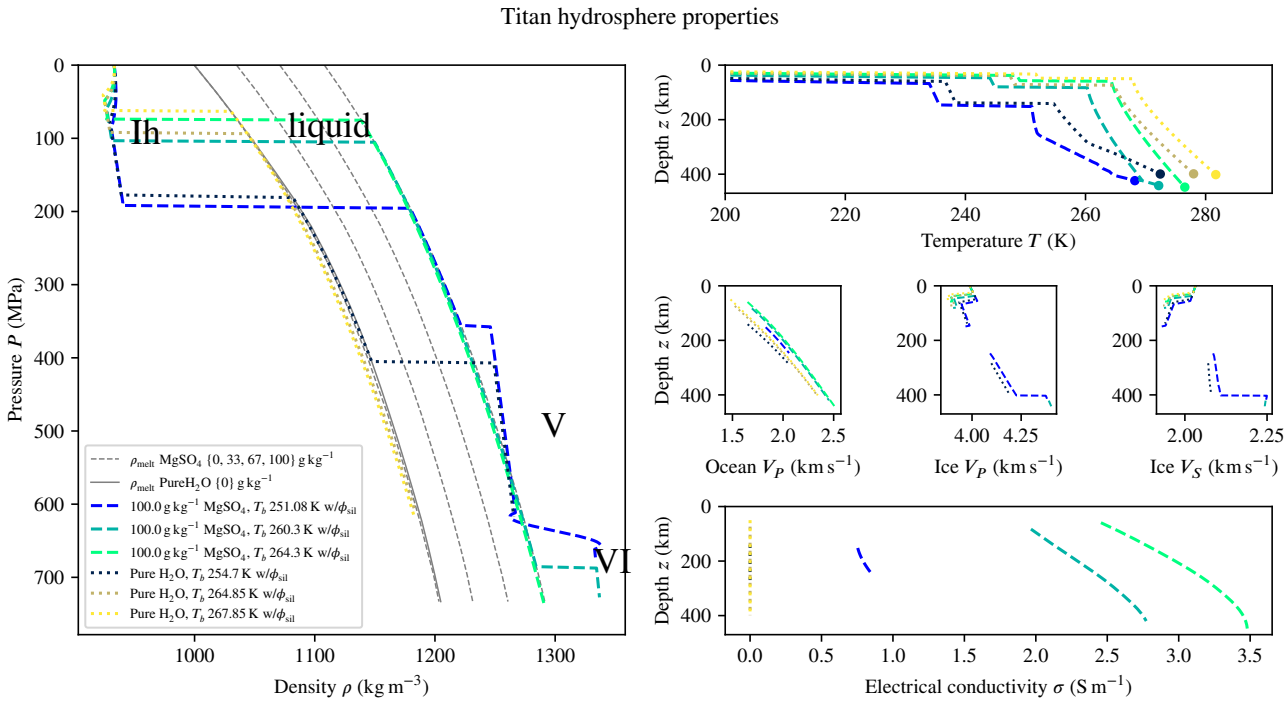

Figure S5. Updated *PlanetProfile* outputs for Titan, modeled after the conditions studied by Vance et al. (2018). Compare to Figure 12 from Vance et al. Refer to Table 5 (main text) for variable definitions.

	Titan	**Titan**	**Titan**	**Titan**	**Titan**	**Titan**
Ocean comp.	100.0 g kg^{-1} $MgSO_4$	100.0 g kg^{-1} $MgSO_4$	100.0 g kg^{-1} $MgSO_4$	Pure H_2O	Pure H_2O	Pure H_2O
M(kg)	1.3452×10^{23}	1.3452×10^{23}	1.3452×10^{23}	1.3452×10^{23}	1.3452×10^{23}	1.3452×10^{23}
$M_{\rm model}$(kg)	1.3447×10^{23}	1.3452×10^{23}	1.3446×10^{23}	1.3451×10^{23}	1.3452×10^{23}	1.3447×10^{23}
C/MR^2	$0.341^{+0.010}_{-0.020}$	$0.341^{+0.010}_{-0.020}$	$0.341^{+0.010}_{-0.020}$	$0.341^{+0.010}_{-0.020}$	$0.341^{+0.010}_{-0.020}$	$0.341^{+0.010}_{-0.020}$
$C_{\rm model}/MR^2$	$0.32721^{+0.00000}_{-0.00053}$	$0.32960^{+0.00000}_{-0.00054}$	$0.33026^{+0.00000}_{-0.00037}$	$0.32567^{+0.00000}_{-0.00049}$	$0.32611^{+0.00000}_{-0.00055}$	$0.32638^{+0.00000}_{-0.00055}$
$\rho_{\rm rock,mean}$(kg m^{-3})	2427	2429	2429	2410	2411	2410
T_b(K)	251.08	260.3	264.3	254.7	264.85	267.85
$q_{\rm surf}$(mW m^{-2})	10.1	16.5	20.8	12.0	20.4	24.8
$q_{\rm con}$(mW m^{-2})	11.4	17.7	21.8	13.4	21.6	25.8
$\eta_{\rm con}$(Pa s)	1.10×10^{15}	5.88×10^{14}	4.33×10^{14}	7.62×10^{14}	3.74×10^{14}	3.12×10^{14}
$D_{\rm Ih}$(km)	151.9	82.8	59.3	140.9	73.8	49.9
$D_{\rm ocean}$(km)	95.8	338.3	389.3	143.1	326.1	352.9
$D_{\rm V}$(km)	155.3	-	-	116.5	-	-
$D_{\rm VI}$(km)	21.7	21.8	-	-	-	-
$\overline{\sigma}_{\rm ocean}$(S m^{-1})	0.8	2.4	3.1	0.0	0.0	0.0
$R_{\rm surf}$(km)	2574.7	2574.7	2574.7	2574.7	2574.7	2574.7
$R_{\rm rock}$(km)	2150.0	2131.9	2126.2	2174.2	2174.9	2172.0
$\phi_{\rm rock}$	0.90	0.90	0.90	0.90	0.90	0.90

Table S5. Updated *PlanetProfile* outputs for Titan, modeled after the conditions studied by Vance et al. (2018). Compare to Table 8 from Vance et al. Refer to Table 5 (main text) for variable definitions.

References

Styczinski, M. J., Vance, S. D., Niesyt, M., Lisitsyn, A., Daswani, M. M., Marusiak, A. G., ... Bryant, A. S. (2022). *vancesteven/PlanetProfile: Fix mantle compositions packaged in release* [Software]. Zenodo. Retrieved from `https://doi.org/10.5281/zenodo.7319838` doi: 10.5281/zenodo.7319838

Vance, S. D. (2017). *vancesteven/PlanetProfile: Release for use in reproducing results submitted to Journal of Geophysical Research - Planets* [Software]. Zenodo. Retrieved from `https://doi.org/10.5281/zenodo.844131` doi: 10.5281/zenodo.844131

Vance, S. D., Panning, M. P., Stähler, S., Cammarano, F., Bills, B. G., Tobie, G., ... Banerdt, B. (2018). Geophysical investigations of habitability in ice-covered ocean worlds. *Journal of Geophysical Research: Planets*, *123*(1), 180–205. doi: 10.1002/2017JE005341